ARTICLE

Bottlebrush Copolymers for Gene Delivery: Influence of Architecture, Charge Density, and Backbone Length on Transfection Efficiency

Received 00th January 20xx,
Accepted 00th January 20xx

DOI: 10.1039/x0xx00000x

Thomas G. Floyd,[a] Ji-Inn Song,[a] Alexia Hapeshi, [a] Sophie Laroque,[a] Matthias Hartlieb,*[d, e] Sébastien Perrier*[a,b,c]

The influence of polymer architecture of polycations on their ability to transfect mammalian cells is probed. Polymer bottle brushes with grafts made from partially hydrolysed poly(2-ethyl-oxazoline) are used while varying the length of the polymer backbone as well as the degree of hydrolysis (cationic charge content). Polyplex formation is investigated via gel electrophoresis, dye-displacement and dynamic light scattering. Bottle brushes show a superior ability to complex pDNA when compared to linear copolymers. Also, nucleic acid release was found to be improved by a graft architecture. Polyplexes based on bottle brush copolymers showed an elongated shape in transmission electron microscopy images. The cytotoxicity against mammalian cells is drastically reduced when a graft architecture is used instead of linear copolymers. Moreover, the best-performing bottle brush copolymer showed a transfection ability comparable with that of linear poly(ethylenimine), the gold standard of polymeric transfection agents, which is used as positive control. In combination with their markedly lowered cytotoxicity, cationic bottle brush copolymers are therefore shown to be a highly promising class of gene delivery vectors.

Introduction

The design of polymeric vectors with low toxicity and high transfection efficiency has long been a goal in gene delivery.[1, 2] Introduced as an alternative to viral and lipid vectors, polymeric vectors have positioned themselves as an easily scalable option with plethora of tuneable properties.[3, 4] However, toxicity associated with cationic polymers and low transfection efficiencies compared with their established counterparts have limited the use of polymers in gene delivery.[5]

One attempt at overcoming these limitations has been the introduction of branched architectures into the structure of the polymeric vector, with many of the established polymers in gene delivery possessing highly branched or dendritic structures.[6] A branched architecture may make these polymers behave differently to their linear counterparts, often with favorable properties such as reduced toxicity.[7, 8] Branched polyethylenimine (bPEI)[9, 10] and poly(amidoamine) (PAMAM) dendrimers[11, 12] have found success in the application of gene delivery, with their prevalence indicating an advantage over linear polymers. For example, the synthesis of bPEI is more straightforward than its linear counterpart, although its architecture is less controlled[13] and PAMAM dendrimers have monodisperse molecular weight distributions.

With increasing control over polymer synthesis, branched architectures such as star, graft, or hyperbranched polymers are now more easily accessible for application to drug and gene delivery.[6] Bottlebrush polymers can imitate some of the beneficial properties of branched polymers and can be synthesized in a highly controlled manner with a high degree of structural variation.[14, 15] In terms of structure, variations of parameters such as graft density, graft length, or backbone length can be used to tune the resulting properties. Furthermore, the placement of the charged units can also be varied, with placement on the backbone or grafts offering different structures, and segmentation of cationic charges affecting self-assembly and membrane interaction.[16] Furthermore, neutral bottlebrush polymers can be used as a prodrug for the delivery of covalently bound nucleotides.[17, 18]

An early example in the use of bottlebrush polymers was reported by Jiang *et al.* who grafted poly((dimethylamino)ethyl methacrylate) (DMAEMA) to a poly(hydroxyethyl methacrylate) (HEMA) backbone with degradable linkages between the backbone and graft.[19] These polymers exhibited significant transfection of plasmid DNA (pDNA) in fibroblast cells (COS-7) and showed a reduced toxicity compared to a linear DMAEMA of similar molecular weight.

[a] *Department of Chemistry, University of Warwick, Gibbet Hill Road, Coventry, CV4 7AL, UK*
[b] *Warwick Medical School, University of Warwick, Gibbet Hill Road, Coventry, CV4 7AL, UK*
[c] *Faculty of Pharmacy and Pharmaceutical Sciences, Monash University, 381 Royal Parade, Parkville, VIC 3052, Australia.*
[d] *Institute of Chemistry, University of Potsdam, Karl-Liebknecht-Straße 24-25, 14476, Potsdam, Germany*
[e] *Fraunhofer Institute for Applied Polymer Research (IAP), Geiselbergstraße 69, Potsdam-Golm, Germany*
** Correspondence to mhartlieb@uni-potsdam.de and s.perrier@warwick.ac.uk*
Electronic Supplementary Information (ESI) available: Experimental procedures, NMR spectra and SEC curves of polymers, Images of Gel Electrophoresis, TEM micrographs, flow cytometry plots, Cell morphology images.
DOI: 10.1039/x0xx00000x

Another study using PDMAEMA grafts was recently published by the group of Reineke.[20] They demonstrated an impressive increase in transfection efficiency when bottle brushes were compared to linear precursors and found an increased ability of graft polymers to transport DNA to the cell nucleus as one of the reasons. However, toxicity seemed unaltered by the change in polymer architecture. Finally, Wang and co-workers demonstrated the importance of hydrophobicity in forming efficient polyplexes by reporting the use of low-charge density bottlebrush copolymers, with the grafts comprised of long alkyl chains. Despite the low-charge density, these polymers exhibited transfection efficiencies comparable to PEI with minimal cytotoxicity.[21]

One way to regulate the specific toxicity of such polymers is to modulate the charge density. A polymeric platform which enables straight forward modification of the cationic charge ratio are poly(2-oxazoline)s (POx).[22-24] This system is a fascinating polymer type in this context, since certain derivatives are highly biocompatible[25-28] and possess shielding abilities similar to poly(ethylene glycol).[29-32] In addition, the acidic hydrolysis of POx leads to linear PEI, a highly potent gene delivery vector.[33] Incomplete hydrolysis can lead to polymers combining biocompatibility and transfection abilities. However, this is usually a trade-off between the two properties.[34, 35]

Several POx bottlebrush-based transfection materials have been reported however in all cases, POx was used for its biocompatible properties to reduce toxicity and shield the cationic moieties, rather than to introduce charge into the polymer.[36-38] POx has been grafted onto a linear cationic polymer backbone to shield charge in several instances or a macromonomer has been prepared and copolymerized with cationic monomers.

The application of poly(2-oxazoline-co-ethylenimine) (P(Ox-co-EI)) copolymers has not been studied with bottlebrush polymers, however, previous work in our group investigated the use of hyperbranched P(Ox-co-EI) copolymers in the transfection of pDNA.[7] It was found that the hyperbranched polymers performed comparably with branched poly(ethylenimine) (bPEI) and a linear analogue in terms of transfection and offered a reduced toxicity. Furthermore, a dependency on the degree of cationic charge in the copolymer was observed, with transfection efficiency increasing with increasing charge density. In a previous study we established a protocol for the efficient production of P(Ox-*co*-EI) bottle brushes by a combination of cationic ring-opening polymerization (CROP), reversible addition-fragmentation chain-transfer (RAFT) polymerization, and acidic hydrolysis.[39] Within the present study, these cationic bottle brush copolymers are probed regarding their potential as transfection agents. Their ability to condense pDNA into polyplexes and then transfect mammalian cells in vitro is extensively studied, with the aim of drawing conclusions on the effect of introducing a bottlebrush architecture.

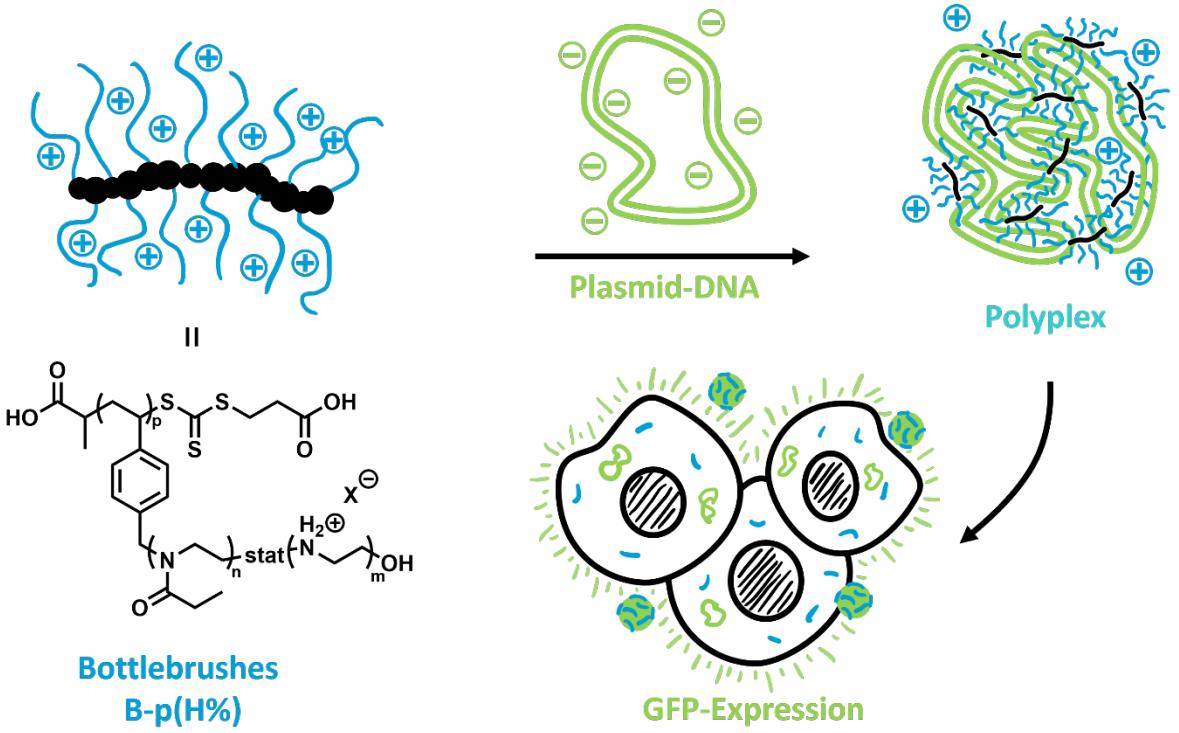

Scheme 1: Overview of bottlebrush copolymer synthesis. H% represents degree of hydrolysis (m/(n+m)); degree of polymerization of side chain (n+m) is 10 for all bottle brushes. Full synthetic details and characterization reported in literature.[39]

Table 1: Composition and characterization data of bottlebrush copolymers partially from a former study.[39]

Polymer	Composition	Hydrolysis (%)	M_n (g mol^{-1})	$Đ$
B-10(32%)	P(EI$_3$-*co*-EtOx$_7$)$_{10}$)	32	7,300	1.24
B-10(46%)	P(EI$_5$-*co*-EtOx$_5$)$_{10}$)	46	7,400	1.17
B-10(69%)	P(EI$_7$-*co*-EtOx$_3$)$_{10}$)	69	9,700	1.19
B-10(78%)	P(EI$_8$-*co*-EtOx$_2$)$_{10}$)	78	10,000	1.13
B-25(67%)	P(EI$_7$-*co*-EtOx$_3$)$_{25}$)	67	15,900	1.16
B-50(67%)	P(EI$_7$-*co*-EtOx$_3$)$_{50}$)	67	25,100	1.32
L-242(81%)	P(EtOx$_{46}$-*co*-EI$_{196}$)	81	13,800*	1.49*

* Determined in aqueous SEC using an aqueous solution of formic acid (0.3%) and NaCl (0.1 mol L^{-1})

Results and Discussion

Bottlebrush Copolymer Synthesis

The synthesis and characterization of cationic bottlebrush polymers has recently been reported by our group.[39] Briefly, a poly(2-ethyl-2-oxazoline) (PEtOx) macromonomer was synthesized *via* the cationic ring-opening polymerization of 2-ethyl-2-oxazoline (EtOx), initiated by 4-vinylbenzyl chloride. This installs a styrenic end-group on the α-terminus of the polymer, capable of undergoing subsequent polymerization to synthesize bottlebrush copolymers. The grafting-through polymerization of the macromonomer was controlled using RAFT polymerization, allowing for influence over the molecular weight and dispersity. Following bottlebrush copolymer formation, EtOx units were hydrolysed in a controlled manner to install a predetermined number of ethylenimine units in the grafts. Kinetic experiments were previously carried out to determine the reaction time required to yield specific degrees of hydrolysis for the bottlebrush polymers. This yielded a series of bottlebrush copolymers with the same graft lengths (DP = 10) but varying backbone lengths and charge densities (Scheme 1, Table 1), which were characterized by aqueous size exclusion chromatography (SEC). The sample names of bottle brushes indicate the nature of the backbone as well as the degree of hydrolysis. For instance, a polymer with a degree of polymerization (DP) of the backbone of 10 and a degree of hydrolysis of 67% is named B-10(67%).

A linear poly (2-oxazoline-*co*-ethylenimine) (P(EtOx-*co*-EI)), L-242(81%), with a molecular weight and charge density similar to B-25(67%) was synthesized to probe the influence of polymer architecture.

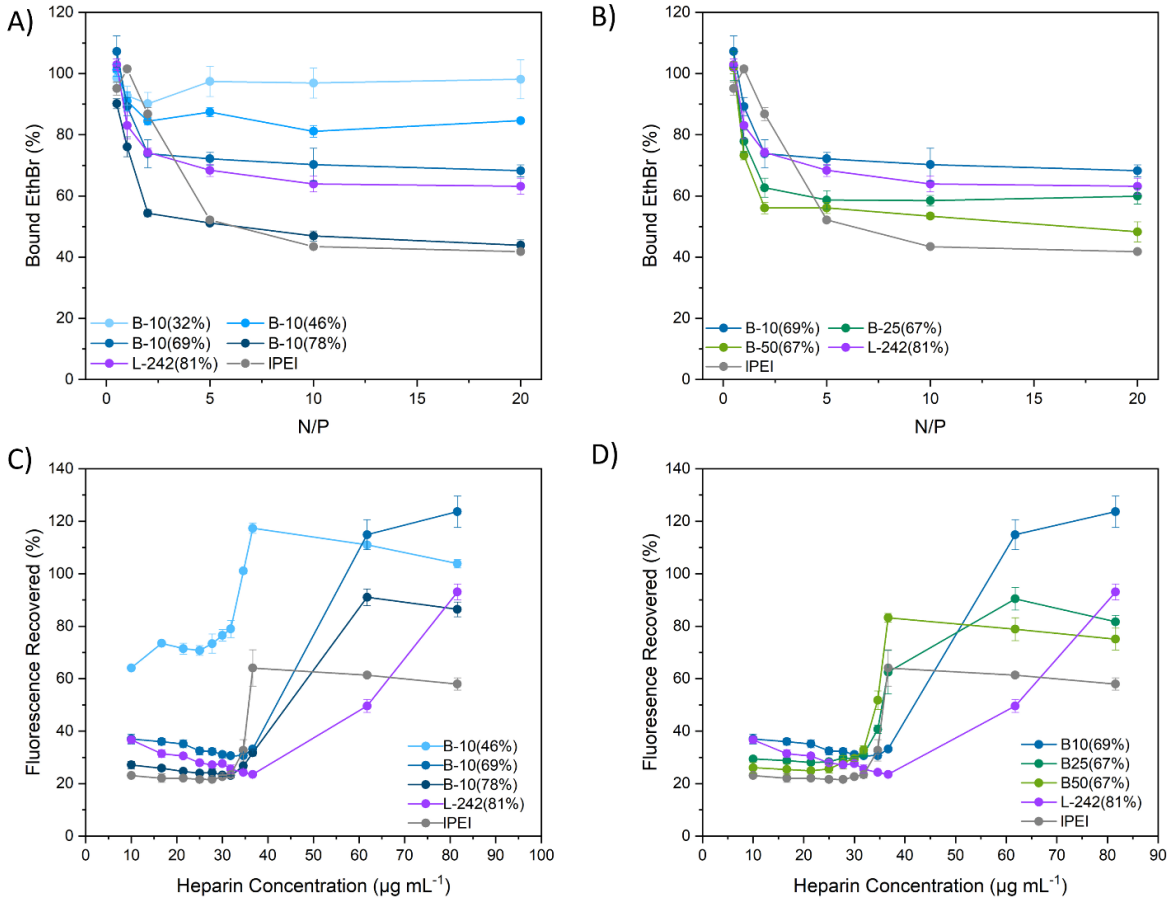

Figure 1: Ethidium bromide displacement assay (A, B) and determination of pDNA released from the polyplex upon incubation with heparin (C, D). A and C compare polymers with increasing charge densities, while B and D compare polymers with different molecular weights and architectures, but similar charge densities.

pDNA Complexation

The ability of bottlebrush copolymers to bind and complex pDNA was investigated using a variety of established assays. This interaction greatly determines how well a polymer will transfect DNA and should allow for selection from polymer library before in vitro experiments. All studies on polyplex formation were carried out using pHR' CMV GFP, a 10.8 kbp plasmid encoding for the enhanced green fluorescent protein (EGFP). Agarose gel electrophoresis was initially used to quantify the N/P ratio required for complete complexation of pDNA by the library of polymers described above (**Table 1**). Polymer and pDNA were mixed at predetermined molar ratios and allowed to incubate at room temperature for 30 minutes. Polyplexes are subsequently loaded into the wells of a 0.8 wt% agarose gel and a voltage applied. Any unbound pDNA will migrate towards the anode, with polyplexes retained in the well.

The data (**Figure S5 – S12**) show that the bottlebrush polymer with 32 % cationic units exhibited very little pDNA binding across a range of N/P ratios (**Figure S5**). Free pDNA was observed in all lanes of the gel indicating the inability of **B-10(32%)** to fully complex pDNA. By increasing the charge density to 46 %, **B-10(46%)**, full complexation of pDNA is achieved at an N/P ratio of 5 (**Figure S6**), and for a bottlebrush polymer with 69 % charge density no free pDNA is observed above an N/P ratio of 2 (**B-10(69%)**, **Figure S7**). Increasing the molecular weight of the polymer whilst retaining similar charge densities did not significantly alter the concentration of polymer required to complex pDNA. Therefore, the complexation of pDNA by bottlebrush polymers appears to primarily be dependent on the cationic charge density of the grafts, with complexation at lower molar ratios observed for polymers with higher charge density. Linear poly(ethylenimine) (25 kDa, lPEI) (**Figure S12**) and **L-242(81%)** (**Figure S11**) were also analyzed and exhibited similar binding efficiencies to the bottlebrush polymers with similar charge densities. From these results, the branched architecture of the polymer does not appear to play a significant role in its ability to complex pDNA.

Polyplex formation can be further studied by determining the displacement of fluorescent intercalating agents, such as ethidium bromide (EthBr), from between the base pairs of double-stranded DNA.[40] Electrostatic binding between the polymer and pDNA causes EthBr to be released, decreasing the overall fluorescence intensity. **Figure 1A** shows the level of EthBr displacement for a series of bottlebrush polymers with the same molecular weight but increasing charge density (from 32 – 81 %). Again, **B-10(32%)** exhibits very little displacement of the EthBr, which correlates with the results from the agarose gel polyplex formation assay. As the charge density increases, higher amounts of EthBr are displaced from within the pDNA, with **B-10(78%)** exhibiting the highest degree of displacement among bottle brushes with 55 % at N/P 20. In this assay, the polymer architecture seems to affect binding as **B-10(78%)** shows a binding capacity similar to that of lPEI and greater than the linear copolymer control (**L-242(81%)**). The comparable linear copolymer reaches a plateau at higher fluorescence values pointing towards an increased dye displacement for bottle brush architectures.

The effect of molecular weight is less pronounced than that of charge density, again in close agreement with the results from agarose gel electrophoresis. A series of bottlebrush polymers with the same charge density and different molecular weight were compared (**Figure 1B**). As the molecular weight increased there is a slight increase in the amount of EthBr displaced, with **B-50(67%)** displacing 20 % more EthBr than **B-10(69%)**. **L-242(81%)** displaces a similar amount of EthBr to the bottlebrush polymer with a corresponding molecular weight (**B-25(67%)**), while possessing a higher charge density. Also, a higher molecular weight brush, **B-50(67%)**, is found to displace even more EthBr than **L-242(81%)** further illustrating the molecular weight dependence of EthBr binding. lPEI exhibits the greatest level of EthBr displacement of all polymers assessed, displacing a maximum of 60 % at N/P 20, which is associated with its high charge density (100%). As **B-10(32%)** exhibited poor complexation with pDNA it was discarded from all further experiments.

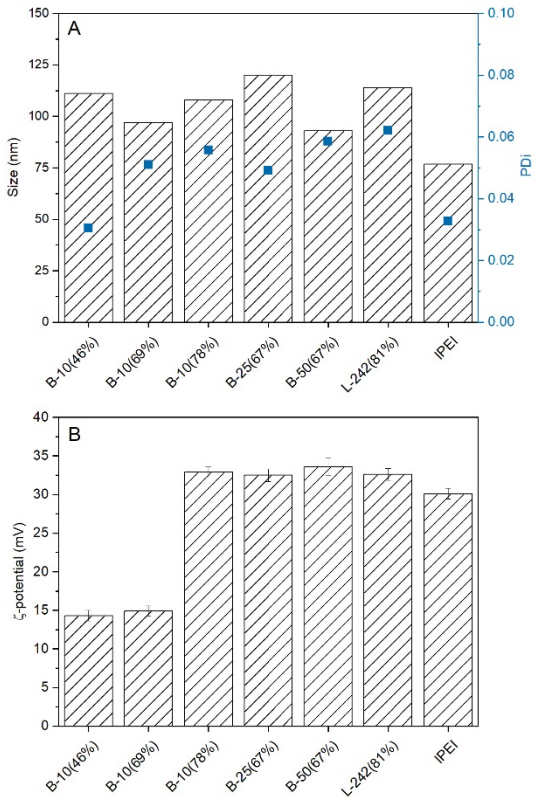

Figure 2: A - Size of polyplexes determined by dynamic light scattering (DLS). Polydispersity index (PDi) calculated using Equation S1. B - Zeta-potential measurements of polyplexes at N/P 20.

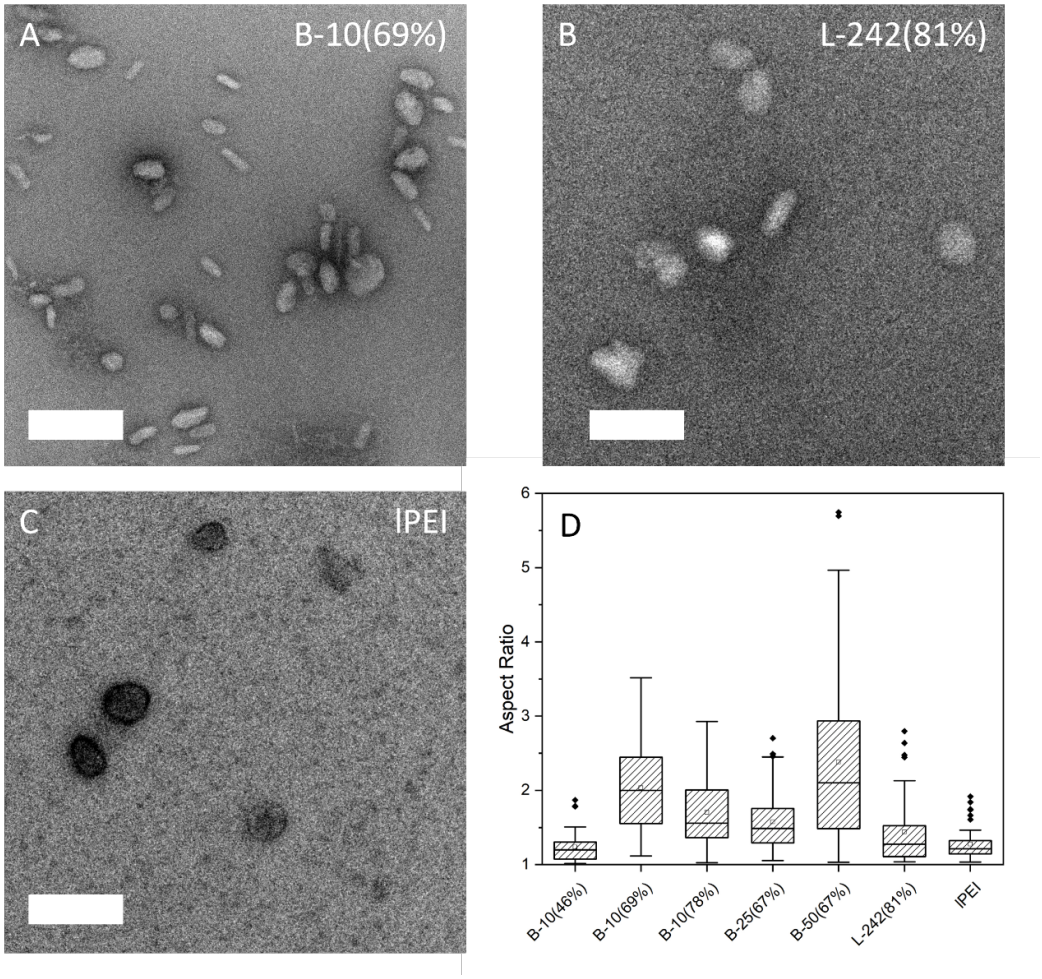

Figure 3: TEM images of polyplexes at N/P = 20 stained with uranyl acetate, Scale bars are 300 nm; A) B-10(69%), B) L-242(81%), C) lPEI; D) Comparison of aspect ratios between formed polyplexes (TEM images and plots of major and minor axis can be found in **Figure S13-S18**).

One barrier for the efficient delivery of pDNA is the competing interactions between the polyplexes and anionic macromolecules, such as glycosaminoglycans (GAGs). These polysaccharides are major components of the extracellular matrix of tissues and can also be found inside cells or on their surface.[41] To study the effects of competitive binding with polyanions, polyplexes in the presence of EthBr were incubated with increasing concentrations of heparin, a highly sulfonated GAG. As heparin displaces pDNA from the complex, EthBr can bind with the pDNA, causing an increase in fluorescence. After each addition of heparin, the fluorescence of the solution was measured and compared to the fluorescence of free pDNA and EthBr.

Figure 1C displays the change in fluorescence for polymers with increasing charge density. Before any addition of heparin, **B-10(45%)** shows a significant level of fluorescence. This corresponds to previous results where the polymer resulted in a lower level of EthBr displacement compared to polymers with greater charge density. A similar concentration of heparin is required for all samples to disrupt the polyplex as indicated by a sharp increase in fluorescence at around 0.35 mg mL^{-1} heparin. This indicates a similar binding strength for all polymers regardless of charge density. The difference could however be below the resolution of the data points. For all partially hydrolyzed samples similar final levels of pDNA displacement are observed, indicating similar stability towards competing anions, while bottle brushes seem to release their payload at lower concentration compared to the liner control. lPEI-based polyplexes seem to be more stable and level off at lower fluorescence values.

Figure 1D shows the level of displacement for bottlebrush copolymers with increasing molecular weights and the linear copolymer and lPEI control. Displacement of pDNA appears to occur at similar heparin concentrations for the bottlebrush copolymers with higher levels of recovered fluorescence observed for lower molecular weight copolymers. The linear copolymer requires a higher concentration of heparin to cause an increase in fluorescence, showing a stronger affinity for pDNA than the bottlebrush copolymers.

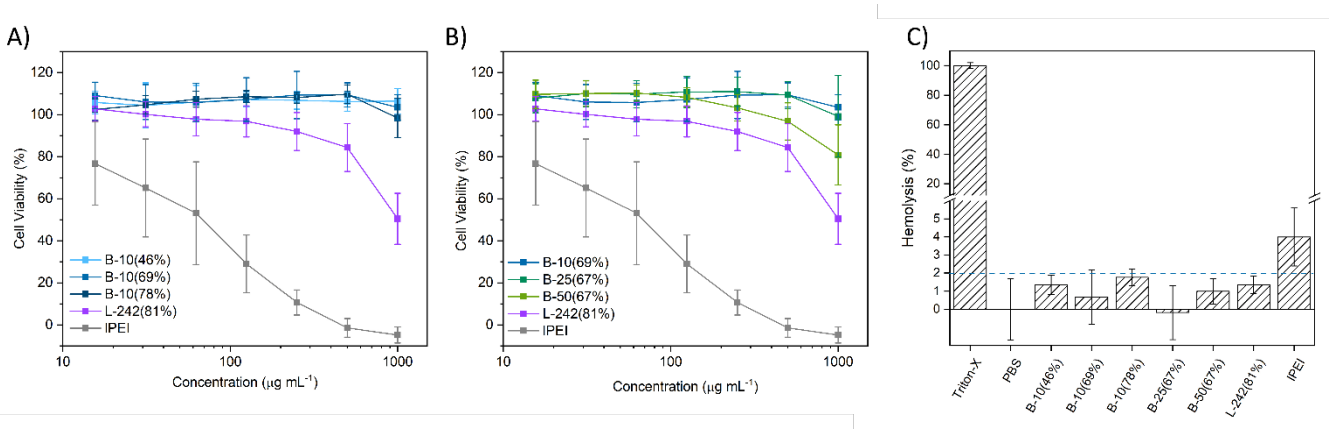

Figure 4 Toxicity of polymers against HEK293T cells (A, B) and sheep red blood cells (C). A) Effect of charge density on HEK293T cell viability, B) Effect of molecular weight and architecture on HEK293T cell viability. C) Hemolysis of polymers against sheep red blood cells.

lPEI appears to withstand displacement to a higher degree than all polymers with a lower level of recovered fluorescence observed at the maximum concentration of heparin administered.

Overall, while gel electrophoresis indicates no significant difference between various architectures, the more sensitive EthBr assay shows stronger binding and easier release of pDNA when complexed with bottle brush copolymers as opposed to linear equivalents. As expected, the charge density affects complexation strongly while overall molecular weight of the polycation plays a subordinate role.

Polyplex Morphology

Cellular uptake of nanoparticles is greatly influenced by their size and morphology, therefore polyplexes were characterized using dynamic light scattering (DLS) and imaged via transmission electron microscopy (TEM). Polyplexes were prepared at an N/P ratio of 20 as described above. By DLS, polyplexes formed from bottlebrush and linear P(Ox-*co*-EI) all had a similar size, in the range of 90 – 120 nm. lPEI was observed to form the smallest polyplex with a diameter of 77 nm (**Figure 2A, Figure S29**). A likely reason is that lPEI has the highest charge density and chain flexibility of the polymers tested. There was little difference in size between the linear and bottlebrush polymers, or any observable trend in size caused by differences in molecular weight and charge density. This is inconsistent with previous work by Cook *et. al.* on hyperbranched systems where a considerable size difference was observed between linear and hyperbranched polymer-based polyplexes.[7] However, the molecular weight of the linear polymer used in this study was much higher, which was shown to influence the resulting size of the polyplex in a study by Bauer *et. al.* where high molecular weight polymers were able to form smaller polyplexes.[34] All polyplexes were observed to have a positive surface potential, between 15 and 35 mV (Figure 2B). The only observed difference was the surface charge of polyplexes formed by **B-10(46%)** and **B-10(69%)**, which exhibited lower zeta-potentials than the other polyplexes. For **B-10(46%)** this could be caused by the lower charge density of the polymer. It is unclear as to why **B-10(69%)** possesses a lower zeta-potential than **B-10(78%)**, given the similarity in charge density and molecular weight.

In addition to size, morphology also effects the interaction of nanoparticles with biological system.[42, 43] To complement the DLS measurements transmission electron microscopy (TEM) was used to determine the morphology of the polyplexes (**Figure 3A-C**). Polyplexes were prepared and deposited onto a formvar/carbon coated grid before staining with uranyl acetate. The major and minor axis of each polyplex was measured for all samples and are plotted in **Figures S17** and **S18**. The aspect ratio, which is the ratio between the major and minor axis was determined and is plotted in **Figure 3D**.

A value close to 1 indicates spherical objects, with an increase in aspect ratio indicating elongated structures. For all bottlebrush polymers, except for **B-10(46%)**, an average aspect ratio > 1.5 was observed, suggesting the formation of elongated structures. This morphology is visualized in the TEM images (**Figure 3A**), which show a mixture of elongated and spherical structures. lPEI, **L-242(81%)**, and **B-10(46%)** exhibit more spherical polyplexes, with an aspect ratio approaching 1. The formation of elongated structures is also observed in a previous study on polyplex formation using oligopeptide bottlebrush copolymers.[44]

Toxicity and Transfection

The toxicity of the polymers against red blood cells and human embryonic kidney cells (HEK293T) was determined. The XTT assay was used to ascertain cell viability of HEK293T cells after incubation with the polymers (Figure 4A-B). Polymers were incubated with HEK293T cells at varying concentrations (15.63 – 1000 μg mL^{-1}) for 24 hours, before their removal and addition of XTT. The cell viability was determined within three independent experiments including three repetitions each. All bottlebrush polymers exhibit neglectable toxicity towards HEK293T cells, with **B-50(67%)** showing the lowest cell viability of 80 % at 1000 μg mL^{-1}. **Figure 4A** compares bottlebrush

copolymers with increasing cationic charge density and identical backbone lengths.

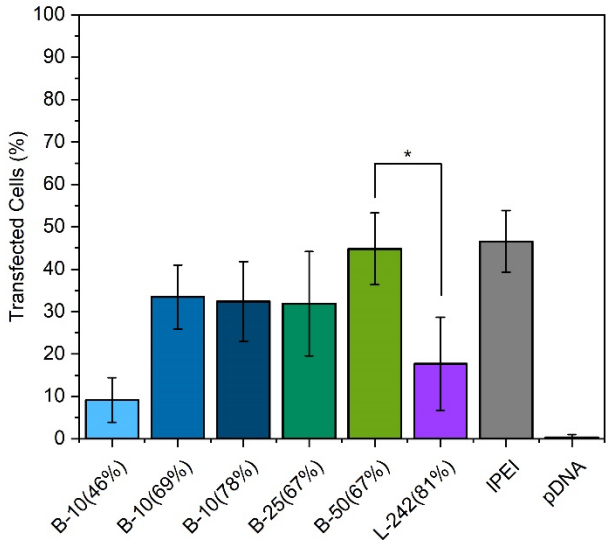

Figure 5 Transfection of HEK293T cells in Opti-MEM reduced serum media using polyplexes (N/P = 20, [pDNA] = 10 μg mL^{-1}) comprised of polymers and a pDNA encoding for EGFP. Expression of EGFP was measured using flow cytometry. Values represent mean ± SD (n = 5). * Significant difference ($p < 0.001$) by ANOVA analysis.

At this molecular weight there is little effect of charge density on the cytotoxicity of the polymers. Keeping the charge density consistent and increasing the molecular weight causes a slight increase in cytotoxicity (Figure 4B). However, the cell viability is still higher than 80 %, which is considered below the threshold for toxic polymers. Comparison of a linear and bottlebrush polymer with similar molecular weights reveals that linear polymers have an increased toxicity compared to their bottlebrush counterparts. lPEI exhibited high toxicity across a range of concentrations, with cell viability below 80 % for all concentrations. While bPEI was not included within this study, previous tests using the same cell line and conditions revealed an even higher toxicity of the branched polycation (<20% of viability at 20 μg mL^{-1}).[7] This further highlights the biocompatibility of the herein presented bottle brushes.

Hemolysis was determined at 37 °C with a polymer concentration range from 8 to 1024 μg mL^{-1} against sheep red blood cells. All investigated bottle brush polymers show a negligible influence on the integrity of erythrocytes (< 2%) while lPEI causes a slight hemolysis (< 5%) (**Figure 4C**).

Taken together, biocompatibility of investigated polymers seems to scale drastically with architecture, with bottle brush copolymers being markedly less toxic compared to a linear counterpart. It should be emphasized that pure polymers instead of polyplexes were investigated regarding their toxicity. The complexation of genetic material and resulting screening of charges could otherwise mask polymer toxicity.[45] Consequently, the herein presented gene delivery system can be regarded as highly biocompatible.

To probe transfection ability, HEK293T cells were transfected with polyplexes formed using a plasmid encoding for EGFP, enabling quantification of transfection as the cells will display fluorescence upon successful protein expression.

During the transfection experiments, aggregates were observed in the wells when viewed under a microscope. These aggregates were found in all wells containing polyplexes, but not in wells containing naked pDNA. To determine the cause of aggregation, polyplexes from **B-10(69%)** and lPEI were incubated within different media and visualized under a microscope to check for aggregation. Polyplexes incubated with fresh Opti-MEM or that taken from the supernatant of growing cells exhibited aggregation, however those incubated in water did not (**Figure S27**). Thus, protein interaction of polyplexes, could hinder successful transfection. However, due to their positive zeta potential, such behavior is in part expected and does not change markedly with polymer architecture.

The transfection ability of bottlebrush copolymers was compared to lPEI (positive control) and naked pDNA (negative control) to determine their ability to transfect HEK293T cells (**Figure 5**). The percentage of cells transfected was determined by flow cytometry, comparing the number of cells exhibiting EGFP fluorescence compared to the total number of cells. In terms of transfection some immediate trends are noticeable. First, bottlebrush polymers with a charge density below 67 % exhibited poor transfection compared to polymers with charge density ≥ 67 %. Comparison of **B-10(46%)** and **B-10(69%)** showed a 3.5 x increase in cells transfected by increasing the charge density from 46 % to 69 %. There was little difference in transfection efficiency between **B-10(69%)** and **B-10(78%)** suggesting a negligible effect in charge density above a certain threshold. With toxicity scaling with the charge density, this a highly promising result as it enables to use less-toxic polymers without sacrificing transfection efficiency, something rarely found in the literature.

Secondly, molecular weight appeared to also play a role in the transfection efficiency of the polyplexes with **B-50(67%)** exhibiting the highest percentage of cells expressing EGFP for all bottlebrush polymers measured, with comparable levels of expression to lPEI. This result is particularly encouraging as the toxicity of **B-50(67%)** is much lower than that of lPEI, making it a promising candidate for wider use in gene delivery.

Lastly, the influence of architecture is visible with **L-242(81%)** exhibiting lower levels of transfection than all bottlebrush polymers, except for the low charge density **B-10(46%)**. Comparing **L-242(81%)** with **B-25(67%)** allows for the determination of architecture effect as these polymers have similar molecular weights. It is evident that the use of a bottlebrush polymer has its advantages over linear polymers as the transfection efficiency is higher and the toxicity lower. Statistical analysis for the bottlebrush and linear copolymers revealed a significant difference between **L-242(81%)** and **B-50(67%)** only. It should also be noted that bPEI under identical conditions only transfected up to 30% of the cells while being significantly more toxic,[7] demonstrating that a change in architecture alone is insufficient for improved overall transfection results. Only, when partially hydrolyzed polymers

are presented in a confined bottle brush architecture, optimal transfection results are obtained.

Summarizing these observations, P(Ox-*co*-EI) bottle brush copolymers appear to be highly promising vectors for gene transfection as they combine the low toxicity of partially hydrolyzed POx with the excellent transfection abilities of linear PEI.

Conclusions

Within this study we investigate how the polymer architecture of partially hydrolyzed poly(2-oxazoline)s influences their ability to transfect cells with pDNA. Bottlebrush copolymers comprising P(EI-*co*-EtOx) grafts are used and the length of the brush backbone, as well as the charge density (degree of hydrolysis) is varied. Their suitability as gene delivery vector is compared to a linear polymer P(EI-co-EtOx) as well as the gold standard linear PEI.

Our findings indicate that polymers possessing a bottle brush architecture show superior pDNA complexation, at lower charge densities, when compared to their linear counterpart. In addition, they also release said pDNA more readily when offered/in the presence of a competing poly(anion). The elongated shape of bottle brushes seems to translate in to polyplexes as well, as they possess an anisotropic morphology. Also, cytotoxicity was found to be lowered when compared to a linear morphology. Finally, transfection efficiency of the best-performing bottle brush copolymers was similar to the gold standard lPEI while the respective linear equivalent showed significantly lower transfection. This, combined with the biocompatible nature renders cationic bottle brush copolymers highly promising non-viral transfection vectors.

Compared to previous studies,[20] it seems that modulating the charge density within the polymer grafts, as well as short graft lengths have additional advantages when utilizing bottle brush copolymers for gene transfection. This study shows that polymer bottle brushes are a scalable and promising alternative to other gene delivery systems.

Author Contribution

The manuscript was written through contributions of all authors. All authors have given approval to the final version of the manuscript.

Conflicts of interest

There are no conflicts to declare.

Acknowledgements

M.H. gratefully acknowledges funding by the DFG (Emmy-Noether-Program, HA 7725/2-1) We are grateful for the polymer characterization RTP (Daniel Lester) for providing use of the following equipment: Dynamic Light Scattering. Anne C. Lehnen is acknowledged for carrying out the aqueous SEC experiments. We acknowledge the Midlands Regional Cryo-EM Facility, hosted at the Warwick Advanced Bioimaging Research Technology Platform, for use of the JEOL 2100Plus, supported by MRC award reference MC_PC_17136. We would like to thank Professor Nick Waterfield, WMS, University of Warwick, for enabling the use of the Leica DMi8 microscope.

References

1. D. W. Pack, A. S. Hoffman, S. Pun and P. S. Stayton, *Nat. Rev. Drug Discov.*, 2005, **4**, 581-593.
2. H. Yin, R. L. Kanasty, A. A. Eltoukhy, A. J. Vegas, J. R. Dorkin and D. G. Anderson, *Nat. Rev. Genet.*, 2014, **15**, 541-555.
3. H. Cabral, K. Miyata, K. Osada and K. Kataoka, *Chem. Rev.*, 2018, **118**, 6844-6892.
4. S. Indermun, M. Govender, P. Kumar, Y. E. Choonara and V. Pillay, in *Stimuli Responsive Polymeric Nanocarriers for Drug Delivery Applications, Volume 1*, eds. A. S. H. Makhlouf and N. Y. Abu-Thabit, Woodhead Publishing, 2018, DOI: https://doi.org/10.1016/B978-0-08-101997-9.00002-3, pp. 43-58.
5. B. D. Monnery, M. Wright, R. Cavill, R. Hoogenboom, S. Shaunak, J. H. G. Steinke and M. Thanou, *Int. J. Pharm.*, 2017, **521**, 249-258.
6. A. B. Cook and S. Perrier, *Adv. Funct. Mater.*, 2020, **30**, 1901001.
7. A. B. Cook, R. Peltier, J. Zhang, P. Gurnani, J. Tanaka, J. A. Burns, R. Dallmann, M. Hartlieb and S. Perrier, *Polym. Chem.*, 2019, **10**, 1202-1212.
8. A. C. Rinkenauer, S. Schubert, A. Traeger and U. S. Schubert, *J. Mater. Chem. B*, 2015, **3**, 7477-7493.
9. W. T. Godbey, M. A. Barry, P. Saggau, K. K. Wu and A. G. Mikos, *J. Biomed. Mater. Res.*, 2000, **51**, 321-328.
10. A. P. Pandey and K. K. Sawant, *Mater. Sci. Eng., C*, 2016, **68**, 904-918.
11. F. Abedi-Gaballu, G. Dehghan, M. Ghaffari, R. Yekta, S. Abbaspour-Ravasjani, B. Baradaran, J. Ezzati Nazhad Dolatabadi and M. R. Hamblin, *Appl. Mater. Today*, 2018, **12**, 177-190.
12. J. D. Eichman, A. U. Bielinska, J. F. Kukowska-Latallo and J. R. Baker, *Pharm. Sci. Technol. Today*, 2000, **3**, 232-245.
13. M. Jager, S. Schubert, S. Ochrimenko, D. Fischer and U. S. Schubert, *Chem. Soc. Rev.*, 2012, **41**, 4755-4767.
14. C. Feng, Y. Li, D. Yang, J. Hu, X. Zhang and X. Huang, *Chem. Soc. Rev.*, 2011, **40**, 1282-1295.
15. R. Verduzco, X. Li, S. L. Pesek and G. E. Stein, *Chem. Soc. Rev.*, 2015, **44**, 2405-2420.
16. S. Laroque, M. Reifarth, M. Sperling, S. Kersting, S. Klöpzig, P. Budach, J. Storsberg and M. Hartlieb, *ACS Appl. Mater. Interfaces*, 2020, **12**, 30052-30065.
17. D. Wang, J. Lin, F. Jia, X. Tan, Y. Wang, X. Sun, X. Cao, F. Che, H. Lu, X. Gao, C. Shimkonis Jackson, Z. Nyoni, X. Lu and K. Zhang, *Sci. Adv.*, 2019, **5**, 9322.
18. F. Jia, X. Lu, D. Wang, X. Cao, X. Tan, H. Lu and K. Zhang, *J. Am. Chem. Soc.*, 2017, **139**, 10605-10608.
19. X. Jiang, M. C. Lok and W. E. Hennink, *Bioconj. Chem.*, 2007, **18**, 2077-2084.

20. R. J. Dalal, R. Kumar, M. Ohnsorg, M. Brown and T. M. Reineke, *ACS Macro Lett.*, 2021, **10**, 886-893.
21. J. O'Keeffe Ahern, S. A, D. Zhou, Y. Gao, J. Lyu, Z. Meng, L. Cutlar, L. Pierucci and W. Wang, *Biomacromolecules*, 2018, **19**, 1410-1415.
22. R. Luxenhofer, Y. Han, A. Schulz, J. Tong, Z. He, A. V. Kabanov and R. Jordan, *Macromol. Rapid Commun.*, 2012, **33**, 1613-1631.
23. V. de la Rosa, *J. Mater. Sci. Mater. Med.*, 2014, **25**, 1211-1225.
24. M. Hartlieb, K. Kempe and U. S. Schubert, *J. Mater. Chem. B*, 2015, **3**, 526-538.
25. J. Kronek, Z. Kroneková, J. Lustoň, E. Paulovičová, L. Paulovičová and B. Mendrek, *J. Mater. Sci. Mater. Med.*, 2011, **22**, 1725-1734.
26. J. Kronek, E. Paulovičová, L. Paulovičová, Z. Kroneková and J. Lustoň, *J. Mater. Sci. Mater. Med.*, 2012, **23**, 1457-1464.
27. R. Luxenhofer, G. Sahay, A. Schulz, D. Alakhova, T. K. Bronich, R. Jordan and A. V. Kabanov, *J. Controlled Release*, 2011, **153**, 73-82.
28. M. Bauer, S. Schroeder, L. Tauhardt, K. Kempe, U. S. Schubert and D. Fischer, *J. Polym. Sci., Part A: Polym. Chem.*, 2013, **51**, 1816-1821.
29. T. Lorson, M. M. Lübtow, E. Wegener, M. S. Haider, S. Borova, D. Nahm, R. Jordan, M. Sokolski-Papkov, A. V. Kabanov and R. Luxenhofer, *Biomaterials*, 2018, **178**, 204-280.
30. L. Wyffels, T. Verbrugghen, B. D. Monnery, M. Glassner, S. Stroobants, R. Hoogenboom and S. Staelens, *J. Controlled Release*, 2016, **235**, 63-71.
31. M. Platen, E. Mathieu, S. Lück, R. Schubel, R. Jordan and S. Pautot, *Biomacromolecules*, 2015, **16**, 1516-1524.
32. M. Glassner, L. Palmieri, B. D. Monnery, T. Verbrugghen, S. Deleye, S. Stroobants, S. Staelens, L. wyffels and R. Hoogenboom, *Biomacromolecules*, 2016, DOI: 10.1021/acs.biomac.6b01392.
33. L. Tauhardt, K. Kempe, K. Knop, E. Altuntaş, M. Jäger, S. Schubert, D. Fischer and U. S. Schubert, *Macromol. Chem. Phys.*, 2011, **212**, 1918-1924.
34. M. Bauer, L. Tauhardt, H. M. L. Lambermont-Thijs, K. Kempe, R. Hoogenboom, U. S. Schubert and D. Fischer, *Eur. J. Pharm. Biopharm.*, 2018, **133**, 112-121.
35. A. K. Blakney, G. Yilmaz, P. F. McKay, C. R. Becer and R. J. Shattock, *Biomacromolecules*, 2018, **19**, 2870-2879.
36. T. von Erlach, S. Zwicker, B. Pidhatika, R. Konradi, M. Textor, H. Hall and T. Lühmann, *Biomaterials*, 2011, **32**, 5291-5303.
37. E. Haladjova, S. Halacheva, D. Momekova, V. Moskova-Doumanova, T. Topouzova-Hristova, K. Mladenova, J. Doumanov, M. Petrova and S. Rangelov, *Macromol. Biosci.*, 2018, **18**, 1700349.
38. A.-K. Trützschler, T. Bus, M. Sahn, A. Traeger, C. Weber and U. S. Schubert, *Biomacromolecules*, 2018, **19**, 2759-2771.
39. T. G. Floyd, S. Häkkinen, S. C. L. Hall, R. M. Dalgliesh, A.-C. Lehnen, M. Hartlieb and S. Perrier, *Macromolecules*, 2021, **54**, 9461-9473.
40. W. C. Tse and D. L. Boger, *Curr. Protoc. Nucleic Acid Chem.*, 2005, **20**, 8.5.1-8.5.11.
41. M. Ruponen, S. Rönkkö, P. Honkakoski, J. Pelkonen, M. Tammi and A. Urtti, *J. Biol. Chem.*, 2001, **276**, 33875-33880.
42. R. Toy, P. M. Peiris, K. B. Ghaghada and E. Karathanasis, *Nanomedicine (London, U. K.)*, 2014, **9**, 121-134.
43. N. Nishiyama, *Nat. Nanotechnol.*, 2007, **2**, 203-204.
44. J. Shi, J. L. Choi, B. Chou, R. N. Johnson, J. G. Schellinger and S. H. Pun, *ACS Nano*, 2013, **7**, 10612-10620.
45. S. Boeckle, K. von Gersdorff, S. van der Piepen, C. Culmsee, E. Wagner and M. Ogris, *J. Gene Med.*, 2004, **6**, 1102-1111.

ARTICLE

TOC Graphic